# Determination of subcell open circuit voltages and $I_{ph}$–$V_{oc}$ curves in multijunction solar cells by sequentially pulsed, monochromatic illumination

M. Rutzinger,[1,2] H. Nesswetter,[1] P. Lugli,[2] A. W. Bett,[3] and C. G. Zimmermann[1]
[1]*Airbus DS, 81663 Munich, Germany*
[2]*Technische Universität München, Arcisstr. 21, 80333 Munich, Germany*
[3]*Fraunhofer Institute for Solar Energy Systems ISE, Heidenhofstr. 2, 79110 Freiburg, Germany*

(Received 17 April 2016; accepted 14 June 2016; published online 24 June 2016)

The open circuit voltages $V_{oc}$ of individual subcells in a multijunction solar cell are measured by illuminating a given subcell with a pulse of spatially homogeneous, nearly monochromatic light with a rising edge in the $\mu$s regime. The influence of luminescent coupling and semi-transparency on $V_{oc}$ is eliminated by over-illuminating all subcells below this subcell with a preceding light pulse. By using a suns-$V_{oc}$ approach, the two-diode model dark saturation currents of each subcell are extracted. The proposed method is verified experimentally as well as through simulations on three and four-junction solar cells. *Published by AIP Publishing.*
[http://dx.doi.org/10.1063/1.4954836]

In multijunction solar cells, only the series connected stack can be contacted externally and thus only the sum of the subcell voltages is directly accessible. Several methods have been proposed to extract the subcell open circuit voltages $V_{oc}$. By using Rau's reciprocity relation,[1] the subcell $V_{oc}$ can be measured with the help of the external quantum efficiency (EQE) and the electroluminescence (EL) spectrum.[2,3] A major drawback of this well established EL-$V_{oc}$ method is that widely used indirect bandgap semiconductors such as Germanium or Silicon have very low light emission rates and thus only current densities above ~0.5 suns are accessible.[3] Alternatively a voltage dependent capacitance analysis has been suggested to extract the subcell $V_{oc}$ by exploiting a change in slope in the capacitance voltage curve.[4]

We recently showed that the subcell $V_{oc}$ can be measured with the help of a ms pulse of illumination which is only absorbed in the subcell of interest.[5] Since in high quality multijunction solar cells, a fraction of the charge carriers recombine radiatively,[6] photocurrent and therefore voltage in the subcell below is generated. By determining the efficiency of this luminescent coupling (LC) effect, its contribution on $V_{oc}$ can be eliminated in a complex set of measurements. The accuracy decreases significantly for a higher number of p-n junctions as the voltage in every subcell below the illuminated one has to be taken into account. In addition, due to the logarithmic dependence of open circuit voltage on photocurrent, even subcells with low LC efficiency generate a considerable $V_{oc}$ contribution. Since low LC efficiency is difficult to measure accurately, this adds further uncertainties.

This letter again relies on the measurement of subcell voltages by pulsed illumination. But instead of using one pulse, all junctions are illuminated essentially at the same time by a series of ms pulses, which are switched on with a time delay of several 10 $\mu$s. The impact of LC onto the open circuit voltages of the lower subcells is minimized in this case and the subcell voltages can be directly read out from the step height in the voltage-time curve. By determining the associated photocurrents in a separate measurement, the implied I-V curve of each subcell can be measured in a suns-$V_{oc}$ fashion.[7]

In order to verify this method and to demonstrate its broad applicability, two different multijunction solar cell types manufactured by AZUR Space were used. First, a four-junction upright metamorphic (4J-UMM) AlInGaP/AlInGaAs/InGaAs// Ge cell,[8] 40 × 80 mm in size with cropped corners, totaling an area of 30.2 $cm^2$ was measured, followed by a 14.2 $cm^2$ GaInP/GaInAs/Ge latticed matched triple-junction cell, labeled 3J-LM. Several cells were measured and the results from representative devices are shown in the following. The individual subcells, starting from the highest band gap, are labeled top, middle, bottom in the three-junction case and J1, J2, J3, and J4 in the four-junction cell.

The experimental setup consisted of a temperature controlled vacuum chuck on which the solar cell under test was contacted with a 4-wire connection. Fiber coupled diode lasers with 1470 nm, 975 nm, and 803 nm as well as a 405 nm light emitting diode (LED) array were used as light sources. These wavelengths are appropriate to illuminate each subcell individually in both cell types, as shown in the plot of the EQE in Fig. 1. Note that the AlInGaAs layer (J2) in the 4J-UMM device is semi-transparent over a wide wavelength range. The

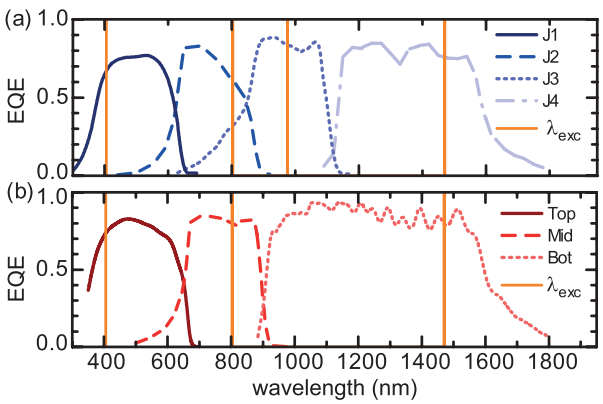


FIG. 1. EQE of the (a) 4J-UMM and (b) 3J-LM cells. The vertical lines mark the excitation wavelengths used in the setup.

semi-transparency (ST), defined as the ratio of the EQE of J3 to the one of J2, is ~52% at the 803 nm laser wavelength.

Each light source was equipped with beam shaping optics based on microlens arrays[9] to illuminate the full cell area with a homogeneity better than 10%. A homogenous illumination is important, since the device is not probed locally like in photoluminescence methods, but only globally via current and voltage measurements at the external terminals. The lasers were switched on in a continuous wave (cw)-mode with a rising edge of ~3 $\mu$s and turned off after 0.7 ms. The voltage was measured between the positive and negative contacts of the solar cell using a high impedance voltage-time logging device with an internal resistance of 1 MΩ. This kept the external measurement current small and hence the entire cell at $V_{oc}$. It is important to note that for cells with high parallel resistance, the discharge of the subcell capacitances can take up to 600 s. Therefore, subsequent measurements have to be delayed by this amount, while keeping the cell in a completely dark environment. Further details of the experimental setup can be found elsewhere.[10]

$V_{oc}^{J4}$ of the lowest subcell can be determined by applying a 1470 nm laser pulse and measuring the voltage step at the onset of the plateau for different laser intensities, as visualized by the solid blue curves in Fig. 2(a). Initially, the small measurement current can flow because of the non-negligible p-n junction capacitance of the non-illuminated subcells.[5] As these subcells become charged, a counter voltage builds up and finally the externally measured voltage approaches zero. This occurs on timescales much longer than 1 ms for the typical capacitances of multijunction cells and is therefore not visible in Fig. 2(a).

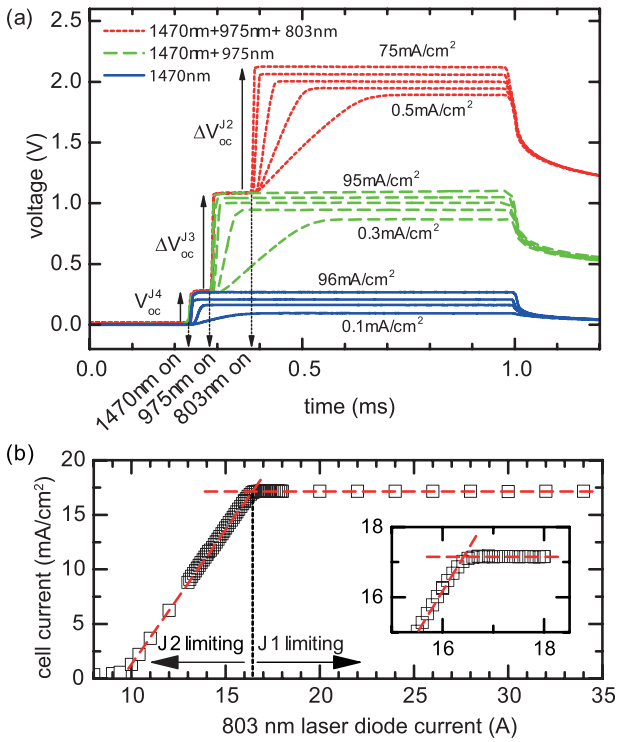


FIG. 2. (a) Pulse sequence for determining $V_{oc}$ of J4 (solid blue line), J3 (dashed green line), and J2 (dotted red line) of a 4J-UMM cell. $\Delta V_{oc}^{n}$ is measured as voltage step from plateau to plateau. (b) Determination of one J2 photocurrent setting by measuring the cell current as a function of the J2 laser current.

Measuring any other than the lowest subcell is complicated by LC as well as by semi-transparent subcells. Both effects induce a photocurrent and, even if it is small, a non-negligible open circuit voltage in the subcell(s) below, while only the sum of the subcell voltages can be measured externally. Therefore, to accurately extract the open circuit voltage $V_{oc}^{n}$ of subcell $n$ only, it is necessary to eliminate the influence of LC and ST. First, all subcells below subcell $n$ are illuminated with a high intensity pulse which generates a voltage plateau. Then, the laser which is primarily absorbed in subcell $n$ is turned on resulting in a voltage step $\Delta V_{oc}^{n}$. According to Eq. (1), this step $\Delta V_{oc}^{n}$ mainly arises from the open circuit voltage of subcell $n$ and also contains a small voltage contribution $\delta V_{oc}^{n+1}$ from the subcell $n+1$ below as the externally generated photocurrent $I_{ph}^{n+1}$ in junction $n+1$ is increased through LC and ST

$$\Delta V_{oc}^{n} = V_{oc}^{n} + \delta V_{oc}^{n+1}, \tag{1}$$

with

$$\delta V_{oc}^{n+1} = V_{oc}^{n+1}(I_{ph}^{n+1} + I_{LC}^{n+1} + I_{ST}^{n+1}) - V_{oc}^{n+1}(I_{ph}^{n+1}). \tag{2}$$

Adding the photocurrents $I_{LC}^{n+1}$ due to LC and $I_{ST}^{n+1}$ due to ST to $I_{ph}^{n+1}$, the increase $\delta V_{oc}^{n+1}$ can be calculated in a one-diode model with ideality factor $\beta$ and dark saturation current $I_{n+1,0}$ of subcell $n+1$ with the help of Eq. (3). $k$, $T$, and $e$ have their usual meaning,

$$\begin{aligned}\delta V_{oc}^{n+1} &= \frac{\beta kT}{e}\left(\ln\frac{I_{ph}^{n+1} + I_{LC}^{n+1} + I_{ST}^{n+1}}{I_{n+1,0}} - \ln\frac{I_{ph}^{n+1}}{I_{n+1,0}}\right),\\ &\approx \frac{\beta kT}{e}\frac{I_{LC}^{n+1} + I_{ST}^{n+1}}{I_{ph}^{n+1}}.\end{aligned} \tag{3}$$

In a worst case estimate, there is only radiative recombination, which implies $\beta = 1$ and a LC efficiency of 100%. For ST a worst case value of 100% is assumed as well. In other words, $I_{ph}^{n+1}$ is increased by $I_{ph}^{n}$ through luminescent coupling and by another contribution of $I_{ph}^{n}$ through semi-transparency. For a ratio $I_{ph}^{n+1}/I_{ph}^{n}$ of 5, which can be achieved easily experimentally, $\delta V_{oc}^{n+1} \approx 10$ mV results. If again a practically unrealistic LC efficiency of 100% is assumed to all subcells below, additional voltage overestimation will originate from these subcells. If the bias light is adjusted such that it generates the same photocurrent $I_{ph}^{n+j}$ in all subcells $n+j$ then in subcell $n+1$ the voltage uncertainty originating from subcell $n+j$ can be calculated similar to Eq. (3), taking into account that LC also increases the photocurrent due to the bias light to $jI_{ph}^{n+1}$. Thus, the voltage uncertainties decrease harmonically and amount to $1/j$ of $\delta V_{oc}^{n+1}$ in subcell $n+j$.

In order to measure $V_{oc}^{J3}$, the 1470 nm laser is turned on first with its maximum intensity. After the open circuit voltage of J4 reaches a plateau, the second laser with a wavelength of 975 nm is turned on with various intensities resulting in the voltage steps $\Delta V_{oc}^{J3}$ as shown by the green, dashed curves in Fig. 2(a). To measure $\Delta V_{oc}^{J2}$, the two lower subcells are illuminated with the maximum intensities possible and

after a plateau, determined by $V_{oc}^{J3}$ and $V_{oc}^{J4}$ is established, the third laser with a wavelength of 803 nm is turned on, which results in the red, dotted curves in Fig. 2(a). From the associated voltage steps, $\Delta V_{oc}^{J2}$ can be read out for each laser intensity. Experimentally, the lasers are turned on with a time delay of $\Delta t \sim 50\ \mu s$ within one consecutive pulse sequence. Finally, the highest bandgap subcell J1 does not need to be measured with pulsed illumination as for this measurement all subcells are illuminated and the measurement current can flow continuously. Therefore, $\Delta V_{oc}^{J1}$ can be obtained by subtracting the known bias voltage generated by the subcells J2–J4 for a given illumination intensity from the voltage obtained with all four light sources turned on.

These sequentially pulsed measurements allow correlating $V_{oc}$ in a junction with a given laser intensity used for that junction. In a second measurement, the laser power is correlated with the photocurrent in the same junction,[5] which results in the photocurrent densities already included in Fig. 2(a). Starting with junction J1, all lower junctions are illuminated with maximum illumination levels. J1 is then brought into current limiting conditions and the photocurrent of J1 can be read out from the measured I-V curve of the cell. To measure the photocurrent of J2, J1 is illuminated such that a chosen photocurrent in J1 results, J3 and J4 are again illuminated with the maximum levels. In Fig. 2(b) the externally measured photocurrent is plotted as a function of the current supplied to the laser illuminating J2. At high J2 illumination levels, the photocurrent is constant, since J1 is current limiting in this case. At a certain cross-over point, the photocurrent decreases with decreasing illumination levels. Exactly at this cross-over point, J1 and J2 are current matched and no luminescent coupling contribution is present. As shown by the inset in Fig. 2(b), the cross-over point is fairly sharp and therefore the externally measured current can be ascribed accurately to a J2 illumination level. A similar procedure is followed for the remaining subcells J3 and J4. In case one subcell is semi-transparent, like J2 in the 4J-UMM cell, an additional illumination component is present in J3. As before, an appropriate illumination level for J3 is determined, which results in current matched conditions without any luminescence coupling contribution into J3. The externally measured current, corrected by the factor (1-ST), then yields $I_{ph}^{J3}$ under the given illumination level.

With the knowledge of subcell photocurrent and open circuit voltage, the implied I-V curve of each subcell can be measured in a suns-$V_{oc}$ fashion.[7] The results obtained for the 4J-UMM cell are illustrated in Fig. 3. For all subcells, the entire range of photocurrents accessible with the experimental setup was measured. The measurement sequence is illustrated graphically in an inset in Fig. 3. The maximum available photocurrent in a lower bandgap subcell was used as biasing current in the pulse sequence for the next subcell. The horizontal lines in the graph denote the $I_{ph}^{n+1}/I_{ph}^{n} \approx 5$ photocurrent criterion assumed for the voltage uncertainty estimate. An ample range of photocurrent is available nevertheless. In this range, each subcell's pulsed-$I_{ph}$-$V_{oc}$ data was fitted according to Eq. (4) with a two diode model using dark saturation currents $I_{01}$ and $I_{02}$

$$I_{ph} = I_{01}\left(\exp\frac{eV_{oc}}{kT} - 1\right) + I_{02}\left(\exp\frac{eV_{oc}}{2kT} - 1\right). \quad (4)$$

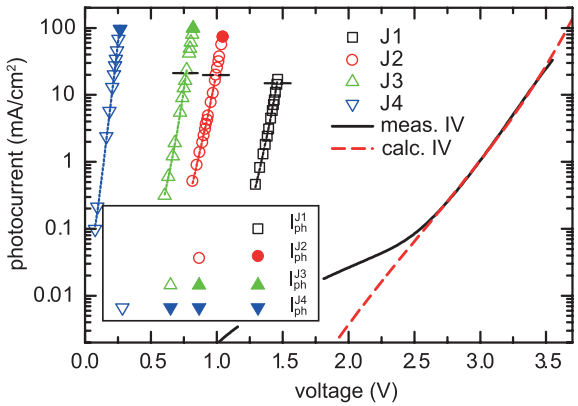


FIG. 3. $I_{ph}$–$V_{oc}$ measurement of the junctions J1-J4 of a 4J-UMM cell. The measured and calculated dark I-V curve is included as well. The inset symbolizes the measurement concept. When moving to the next subcell, the subcells below are illuminated with the maximum intensity.

The resulting fit curves are included in Fig. 3 as well and the dark saturation currents obtained are listed in Table I. As an independent verification, the dark I-V curve of this cell has been calculated based on the dark saturation currents in Table I, with the help of the circuit simulator SPICE.[11] Except for the deviation at low currents, which is due to a parallel resistance, an excellent match is obtained.

The same measurement procedure was also applied to a lattice matched triple junction cell. The subcell pulsed-$I_{ph}$-$V_{oc}$ data obtained is shown in Fig. 4 and the dark saturation currents that were extracted are summarized in Table II. In this case, the dark I-V curve is reproduced very well down to current densities of $10^{-4}$ mA/cm$^2$ due to the higher parallel resistance of this cell.

In order to quantify the errors in the voltage measurement introduced due to LC for a realistic case, this triple junction cell was simulated in SPICE. For the dark saturation currents, the measured values from Table II were used. This ignores the fact that the dark saturation currents in the simulation contain the experimental measurement uncertainty already. For this error estimate, however, it is justified, in particular, in the light of the fact, that the dark I-V curve is accurately reproduced. The LC efficiencies of the cell were determined in a separate measurement according to the method in Ref. 12. The LC efficiency from top to middle cell was 7% and 36% from middle to bottom cell. Subcell capacitance in the 0.1 $\mu$F/cm$^2$ range[5] was also introduced in the SPICE model.

In SPICE, the entire pulse sequence was simulated. Thus, the change in the voltage plateaus due to luminescent coupling and therefore the over-estimation of $V_{oc}^{n}$, could be extracted directly. The results are summarized in Table III.

TABLE I. Dark saturation current densities ($I_{01}$, $I_{02}$) obtained for the 4J-UMM cell.

| 4J-UMM | $I_{01}$ (mA/cm$^2$) | $I_{02}$ (mA/cm$^2$) |
|---|---|---|
| J1 | $1.7 \times 10^{-24}$ | $5.5 \times 10^{-12}$ |
| J2 | $1.1 \times 10^{-16}$ | $6.6 \times 10^{-8}$ |
| J3 | $1.8 \times 10^{-12}$ | $2.5 \times 10^{-6}$ |
| J4 | $3.7 \times 10^{-3}$ | $7.9 \times 10^{-3}$ |

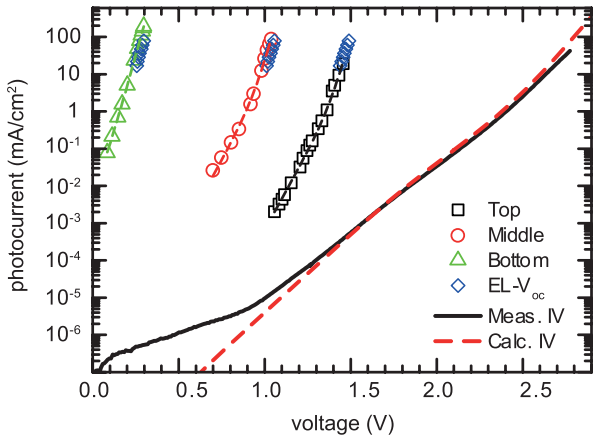


FIG. 4. Measured subcell $I_{ph}$-$V_{oc}$ data of the 3J-LM cell. The simulated dark I-V curve, based on the measured subcell dark saturation currents, fits the measured dark I-V curves very well. The subcell I-V curves measured with help of the EL-$V_{oc}$ method are included for comparison.

TABLE II. Dark saturation current densities ($I_{01}$, $I_{02}$) obtained for the 3J-LM cell.

| 3J-LM | $I_{01}$ (mA/cm$^2$) | $I_{02}$ (mA/cm$^2$) |
|---|---|---|
| Top | $3.7 \times 10^{-24}$ | $5.0 \times 10^{-12}$ |
| Middle | $2.0 \times 10^{-16}$ | $2.6 \times 10^{-8}$ |
| Bottom | $1.8 \times 10^{-3}$ | $3.3 \times 10^{-3}$ |

TABLE III. Simulated voltage over-estimation $\delta V_{oc}^{n}$ for the 3J-LM cell.

| n | Bias (mA/cm$^2$) | $I_{ph}^{n}$ (mA/cm$^2$) | 1 | 20 | 100 |
|---|---|---|---|---|---|
| Mid | $I_{ph}^{bot} = 97$ | $\delta V_{oc}^{mid}$ (mV) | 0.02 | 1.2 | 7.0 |
| Top | $I_{ph}^{mid} = 96$, $I_{ph}^{bot} = 97$ | $\delta V_{oc}^{top}$ (mV) | 0.002 | 0.3 | n/a |

For the top cell, which in reality could only be measured up to a photocurrent of 20 mA/cm$^2$ due to the limitations of the LED array the measurement errors are in the $\mu$V range, in line with the low LC efficiency from the top cell to the junctions below. For the middle cell, the voltage over-estimation is 1.2 mV at a current density of 20 mA/cm$^2$, which amounts to approximately 1/5th of the bottom cell current. This is significantly smaller than the 10 mV resulting from the worst case estimate. For higher middle cell illuminations, the voltage uncertainty increases up to 7.0 mV at a current density of 100 mA/cm$^2$. For fitting of the subcell dark saturation currents to the subcell data, the measurement range up to 1/5th of the current density of the bias illumination is more than sufficient. The voltage uncertainty in this range affects the dark saturation currents $I_{01}$ and $I_{02}$ of the middle cell by less than 5%. The subcell I-V curves were also measured with the help of the EL-$V_{oc}$ method,[3] as illustrated in Fig. 4. The measurements agree very well within ≈10 mV.

In summary, the open circuit voltages of individual subcells can be measured accurately by using pulsed, spatially homogeneous, monochromatic illumination. Appropriate rise times are in the $\mu$s range and the total pulse duration is around 1 ms. The impact of luminescent coupling on $V_{oc}$ of the subcells below is virtually eliminated by jointly illuminating all subcells using a series of pulses which are switched on with a time delay of several 10 $\mu$s. In this sequential scheme, a high intensity light bias is applied to all subcells below the measured subcell. For actual devices, the biggest uncertainty arises from semi-transparent subcells. There measurement errors are introduced both in the determination of the photocurrent for the $I_{ph}$-$V_{oc}$ fit, which is corrected based on EQE data, as well as in the voltage measurement. The latter uncertainty, however, can be reduced to acceptable values, similar to luminescence coupling contributions, by choosing a sufficiently high light bias for the subcells below. Experimentally, there is also the option to choose the illumination wavelength in order to minimize the effect of semi-transparency for a given device design. A specific advantage of the proposed method, compared to the EL-$V_{oc}$ approach, is the extension of the measurement range by almost two orders of magnitude down to ≈0.1 mA/cm$^2$. In addition, it does not rely on the measurement of radiative emissions and is therefore expected to be particular useful for the analysis of multijunction cells irradiated with high particle fluences.

The authors are grateful to D. Lackner for providing the EL-$V_{oc}$ data.

[1]U. Rau, Phys. Rev. B **76**, 085303 (2007).
[2]T. Kirchartz, U. Rau, M. Hermle, A. W. Bett, A. Helbig, and J. H. Werner, Appl. Phys. Lett. **92**, 123502 (2008).
[3]S. Roensch, R. Hoheisel, F. Dimroth, and A. W. Bett, Appl. Phys. Lett. **98**, 251113 (2011).
[4]R. Hoheisel, M. Schachtner, E. Stämmler, and A. W. Bett, Appl. Phys. Lett. **98**, 251106 (2011).
[5]H. Nesswetter, N. R. Jost, P. Lugli, A. W. Bett, and C. G. Zimmermann, Appl. Phys. Lett. **106**, 023903 (2015).
[6]M. A. Steiner and J. F. Geisz, Appl. Phys. Lett. **100**, 251106 (2012).
[7]R. Sinton and A. Cuevas, Appl. Phys. Lett. **69**, 2510 (1996).
[8]G. Strobl, L. Ebel, D. Fuhrmann, W. Guter, R. Kern, V. Khorenko, W. Kostler, and M. Meusel, in *IEEE 40th Photovoltaic Specialists Conference* (IEEE, 2014), pp. 3595–3600.
[9]O. Homburg, T. Mitra, and L. Aschke, Proc. SPIE **7579**, 75790O (2010).
[10]H. Nesswetter, P. Lugli, A. W. Bett, and C. G. Zimmermann, IEEE J. Photovoltaics **3**, 353 (2013).
[11]L. W. Nagel and D. O. Pederson, "SPICE (Simulation Program with Integrated Circuit Emphasis)," Technical Report No. UCB/ERL M382, EECS Department, University of California, Berkeley, 1973.
[12]H. Nesswetter, N. R. Jost, P. Lugli, A. W. Bett, and C. G. Zimmermann, Prog. Photovoltaics **24**, 760 (2016).